Journal of Multidisciplinary Engineering Science and Technology (JMEST)
ISSN: 2458-9403
Vol. 12 Issue 7, July - 2025

Multibody Dynamic Modelling Of Complex Wind Turbine Blade Lightning Protection Systems

Godson I. Ikhazuangbe[1], Osawaru N. Osarimwian[2], F.O. Phillip-Kpae[3], Wocha Chikagbum[4], Maxwell Peppel[5].

[1]Department of Electrical and Electronic Engineering. The University of Nottingham United Kingdom

[2]Institute for Energy Studies, Department of Energy Engineering, University of North Dakota USA

[3]Department of Electrical and Electronic Engineering, Rives State University Port Harcourt, Nigeria

[4]Department of Urban and Regional Planning, School of Environmental Sciences, Ken Saro-Wiwa Polytechnic, Bori, Nigeria

[5]Department of Electrical/Electronic Engineering, Ken Saro-Wiwa Polytechnic, Bori, Nigeria

Abstract- ***Increasing wind turbine sizes get attractive to lightning attacks. Due to unpredictable nature of lightning, accurate data for analysis has been a serious concern for modern wind turbines. Compared to simple structure, lightning interactions with large wind turbines have given rise to complex systems requiring multibody analysis. Research has shown that the maximum electric field strength distributed on the surface of the wind turbine and the surrounding air is very important in determining the point of inception of upward leader and would help in improving lightning protection systems. In contrast to static objects, maximum electric field strength required for the inception of upward leader from wind turbine changes majorly due to blade rotation and certain blade conditions such as; polluted blade surface, varying receptor sizes, receptor positions on the wind turbine, types and shapes of protection method. Maximum electric field variations due to these blade conditions has not been considered well in literature. Analyzing the maximum electric field strength and conducting experimental test on full scale wind turbine is presently very difficult due to height constraint and lack of suitable equipment. In this paper, multibody of complex wind turbine lightning protection systems is modelled considering; various receptor sizes, discrete receptor positions, various lightning protection systems, effect of polluted blade surface, full scale blade length as well as scaled blade tip. The vertical tri-pole cloud charge distribution model is adopted using comsol multiphysics and then evaluated with high voltage strike attachment test. The proposed models can be used to analyze multibodies (various blade conditions) that can affect the inception of upward leader from wind turbines and can be used to analyze longer blades. Dynamically, the blades are rotated***

Keywords—Wind Turbine, Lightning Protection, FEM, Renewable Energy

1. Introduction

Lightning is a universal problem. Between 1992 and 1995, 393 events of lightning damage to wind turbines was reported in Germany alone [1] . When lightning strike attaches to the body of the wind turbine instead of the protection device, the blade and even, the entire wind turbine can be destroyed causing downtimes, loss of wind turbine, and high cost of repair. Modern wind turbines due to their increasing height are now more vulnerable to increased number of lightning strikes. When lightning strikes a wind turbine, resulting damage could be by direct strike or by producing electric and magnetic fields that can induce voltages in local wiring. Damages vary in magnitude, worst with unprotected blades and can be eradicated or reduced by efficient protection system. These systems are usually installed on modern wind turbines [2-5]. It includes; a network of air terminals, bonding conductors, and ground electrodes, designed to provide a low impedance path to ground for possible lightning strikes [6]. Lightning protection problems were well addressed for static objects and Lightning Protection Systems (LPS) are usually fitted on wind turbines by applying the Electro Geometric Model (EGM) methods. The EGM relates the striking distance to the prospective peak stroke current. However, these methods are now invalidated and according to IEC 61400-24 standards, the EGMs are no longer suitable for large wind turbine blades.

Lightning can either be downward initiated or upward initiated. In the presence of a thundercloud, tall wind turbines are increasingly exposed to upward lightning attachment triggered by the wind turbine itself [1, 7-9]. Report shows that upward lightning flashes are initiated or incepted from the enhancement of the electric field produced by thundercloud charge or close lightning discharges [7, 10]. However, the maximum electric field strength required for the initiation of upward leaders from wind turbines is highly dependent on the blade condition and upward leader models are still being investigated. For upward propagating lightning from wind turbine, as mentioned above, the electric field in the air is near

uniform being produced by the cloud and not by a stepped leader. Therefore, for upward leader formation, the strong influence of the stepped leader position is eliminated, and the formation will be dominated by the wind turbine geometry and the electric field distribution.

Lightning strike frequency, point of lightning attachment and lightning protection systems has been evaluated based on downward initiated lightning. However, these might not be effective for upward lightning. Research has shown that the maximum electric field strength distributed on the surface of the wind turbine and the surrounding air is very important in determining the point of inception of upward leader and would help in improving lightning protection systems. In contrast to static objects, maximum electric field strength required for the inception of upward leader from wind turbine changes majorly due to blade rotation and certain blade conditions such as; polluted blade surface, varying receptor sizes, receptor positions and type of protection method.

Maximum electric field variations due to these blade conditions has not been considered in literature. Analyzing the maximum electric field strength and conducting experimental test on full scale wind turbine is presently very difficult due to height constraint and lack of suitable equipment. As power demand and size of wind turbine is in the increase, investigating the variations in maximum electric field strength required for the inception of upward leader from wind turbine due to varying blade conditions has become inevitable. In this paper, multibodies of complex wind turbine lightning protection systems is designed and modelled considering; various receptor sizes, discrete receptor positions, various lightning protection systems, effect of polluted blade surface, full scale blade length as well as scaled blade tip. The vertical tri-pole cloud charge distribution model is adopted using comsol multiphysics.

The extended vertical tri-pole cloud charge distribution model made from two positive charges and a negative charge representing the idealized gross charge structure of a thundercloud is used to create an ambient field representing uniform electric field due to cloud charge distribution at 200 m above ground [11, 12]. The numerical model is developed with finite element analysis; COMSOL Multiphysics. The extended model [11, 12] is applied to a 3D electrostatics model of a full-scale wind turbine; Vestas V100 with 2 MW rated power, 164 m rotor diameter and 49 m long blade. As the blade is rotated, the variations in maximum electric field strength required for the initiation of upward leader is obtained. The thundercloud model was simulated and then evaluated with high voltage strike attachment test experiment in [12].

This work forms a platform for further investigation on modern wind turbines with regard to protecting long blades from lightning.

2. Multibody dynamic models and analysis

In multibody analysis, various models for analyzing blade conditions are presented. They are designed in COMSOL Multiphysics. These includes; model for analyzing thundercloud, model for analyzing wind turbine and thundercloud interface, model for analyzing full scale and small blade tip, model for analyzing rotation, model for analyzing receptor positions, model for analyzing receptor sizes, model for analyzing receptor types and model for analyzing polluted blade surfaces.

2.1 Material Content for the Design

The materials used for the turbine blade, air, thundercloud, the lightning protection systems and ground model's designs are shown in tables 1, 2, 3 and 4 respectively

Table 1 Material used for Turbine blade design

Property	Name	Value	Unit	Property Group
Relative permittivity	Epsilon	4	1	Basic
Relative permeability	Mur	1	1	Basic
Density	Rho	2200[kg/m^3]	kg/m^3	Basic
Electrical conductivity	Sigma	$1.0x10^{-14}$[s/m]	s/m	Basic
Thermal conductivity	K	1.1[w/(m*k)]	w/(m*k)	Basic
Heat capacity at constant pressure	C_p	480[J/(kg*k)]	J/(kg*k)	Basic
Refractive index	N	1.5	1	Refractive index
Refractive index, imaginary part	Ki	0	1	Refractive index
Young's modulus	E	$74X10^9$[pa]	Pa	Young's modulus and Poisson's ratio
Poisson's ratio	Nu	0.3	1	Young's modulus and Poisson's ratio

Table 2 Materials used for thunder cloud and lightning protection systems designs

Property	Name	Value	Unit	Property Group
Electrical conductivity	Sigma	5.998x10^{7}[s/m]	s/m	Basic
Coefficient of thermal expansion	Alpha	17x10^{6}[1/k]	1/k	Basic
Heat capacity at constant pressure	C_p	385[J/(kg*k)]	J/(kg*k)	Basic
Density	Rho	8700[kg/m^3]	kg/m^3	Basic
Thermal conductivity	K	400[w/(m*k)]	w/(m*k)	Basic
Young's modulus	E	110X10^{9}[pa]	Pa	Young's modulus and Poisson's ratio
Poisson's ratio	Nu	0.35	1	Young's modulus and Poisson's ratio
Reference resistivity	Rho0	1.72x108[ohm*m]	Ω*m	Linearized resistivity
Resistivity temperature coefficient	Alpha	0.0039[1/k]	1/k	Linearized resistivity
Reference temperature	Tref	298[k]	K	Linearized resistivity

Table 3 Materials used for Air as the environment

Property	Name	Value	Unit	Property Group
Relative permittivity	epsilonr	1	1	Basic
Relative permeability	Mur	1	1	Basic
Ratio of specific heat	gamma	1.4	1	Basic
Electrical conductivity	Sigma	0[s/m]	s/m	Basic
Dynamic viscosity	Mu	Eta(T[1/K])[pa*s]	Pa*s	Basic
Density	Rho	Rho(Pa[1/pa],T[1/k])[kg/m^3]	kg/m^3	Basic

Table 4 Material used for a perfectly conducting ground (an ideal ground) design

Property	Name	Value	Unit	Property Group
Relative permittivity	Epsilon	1	1	Basic
Relative permeability	Mur	1	1	Basic
Electrical conductivity	Sigma	5.998x10^{-7}[s/m]	s/m	Basic
Coefficient of thermal expansion	Alpha	17e^{-6} (1/k)	(1/k)	Basic
Heat capacity at constant pressure	C_p	385[J/(kg*k)]	J/(kg*k)	Basic
Density	Rho	8700[kg/m^3]	kg/m^3	Basic
Thermal conductivity	K	400[w/(m*k)]	w/(m*k)	Basic
Young's modulus	E	110e^{-9}[pa]	Pa	Young's modulus and Poisson's ratio
Poisson's ratio	Nu	0.35	1	Young's modulus and Poisson's ratio
Reference resistivity	Rho0	1.72e^{-8}[ohm*m]	Ω*m	Linearized resistivity
Resistivity temperature coefficient	Alpha	0.0039[1/k]	1/k	Linearized resistivity
Reference temperature	Tref	298[k]	K	Linearized resistivity

2.2. Model for analyzing thundercloud

The charge structure in a thundercloud is usually replicated by three vertical stacked point charges or spherically symmetrical charge volumes. It consists of a vertical tri-pole made from a negative charge and two positive charges. A summary of various cloud models have been listed in [13, 14]. The cloud model that has been implemented and simulated in this work is taken from [13]. The model is illustrated in Figure 1, it has positive charge at the top, negative in the middle, and a smaller positive at the bottom, and the ground modeled as a perfect conductor. The top two charges are also called the main charges and are usually specified to be equal in magnitude. Sometimes, the lower positive charge is not present. The top two charges form a dipole, said to be positive because the positive charge is above the negative charge, this gives an upward-directed dipole moment. In the simulation, the three charges of +40C, -40C and 3C are placed at height of 12, 7 and 2 km from the ground respectively and modelled as spheres of radii 900m for the 40C charges and 150 m for the charge of 3C [13, 15]. The size of the spheres is such that during meshing, the accuracy of the electric field in the area of interest within the model is ensured.

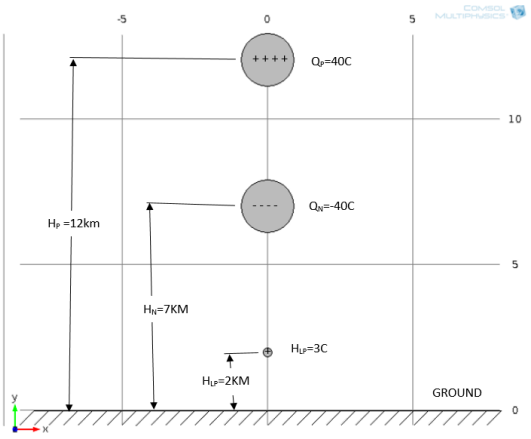

Figure 1: A vertical tri-pole made from two positive charges and a negative charge representing the idealized gross charge structure of a thundercloud. [12]

Where Q_p is the main positive charge, Q_N is the main negative charge, H_{LP} is the lower positive charge and H_P, H_N and H_{LP} are their various distances (in kilometer) from ground.

2.3. model for analyzing wind turbine and thundercloud interface

An increased electric field at ground level produced by the electrical charge within a thundercloud can result in the production of upward leaders from a structure before the formation of a stepped leader. The attachment point is determined by these formation points of these upward leaders.

The results of the electric field at ground from the system of three charges shown in Figure 1 agrees with the report in [13], with maximum ambient field of just over 5kV/m. These values are used in this work and an upward-directed electric field is defined as positive [13].

In order to analyze the maximum electric field strength required for the initiation of upward leaders from wind turbines, the information from the cloud model is combined with the wind turbine model in the simulation. As mentioned above, the vertical tri-pole cloud charge distribution model is used to create an ambient field representing a uniform electric field due to cloud charge distribution at 200 m above ground. A uniform electric field produced by a plane electrode located 200 m above the ground is then applied on the wind turbine model. The magnitude of the applied electric field is 1MV/m (200 X 5KV/m = 1000000V/m). This is based on the results found from Malan's charged cloud model [13]. Figure 2 shows the simulation model. The electrode's polarity is negative; the environment is modeled as air and the wind turbine is sited on the ground. The dimension of the electrode is large enough to prevent flashover from the edges.

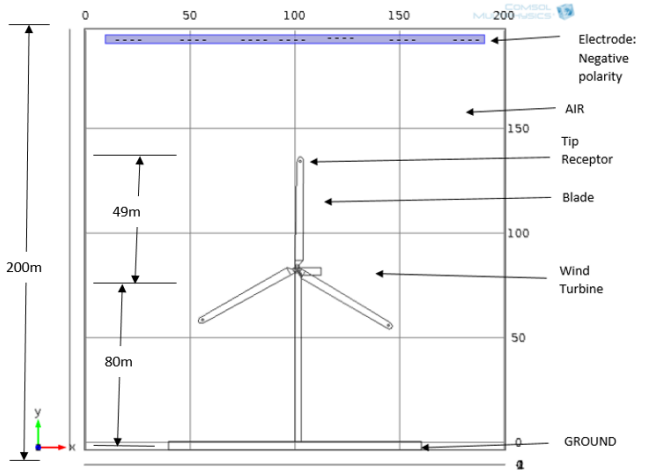

Figure 2: simulation model

a. Wind Turbine Model

The wind turbine used in this study is Vestas V100 with 2 MW rated power, 100 m rotor diameter, swept area 7.854m^2 and 49 m long blade. V100 is a horizontal axis wind turbine with three blades. The blade is made of fibred glass with a relative permittivity: of 4.2, conductivity:1.0×10^{-14} S/m, blade thickness: 10 cm, chamber length: 0.9 m, maximum chord 3.9 m (varied at blade root and tip). The wind turbine nacelle and tower are conductive and are set to ground potential. Hub height (height from the lowest part of the tower to the Centre of the hub) is 80 m. The tower is tubular steel type. The nacelle is 10.4 m long and 3.5 m wide. V100 is shown below in Figure 3

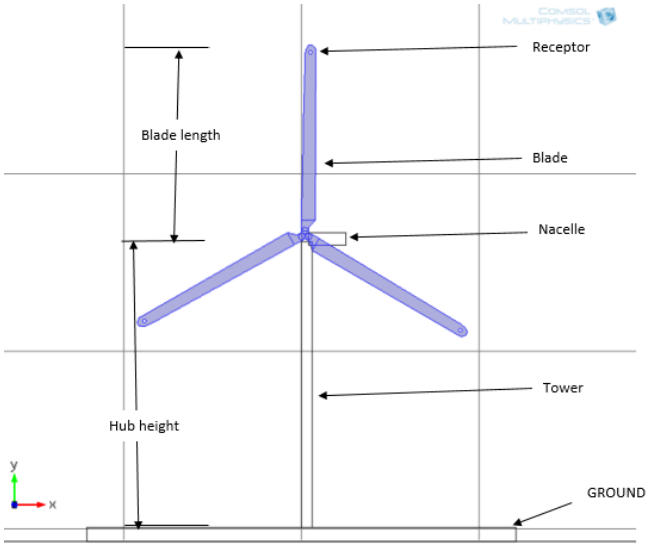

Figure **Error! No text of specified style in document.**: Wind turbine model

2.4. Model for analyzing full scale and small blade tip

To ensure safety against lightning of wind turbines, high-voltage strike attachment tests specified in IEC 61400-24 are adopted to determine points of lightning attachments. These tests are usually conducted with a small blade sample as a representative of the full-scale blade length. However, incidents of lightning

damage to wind turbines are still high, which indicates that small blade samples may not be an adequate representation of full-scale blade. How well these two compare has been a subject of research. Full scale and small blade tip models are presented here and used to compare the maximum electric field strength around a full scale blade and that of a 3m blade tip section to show how they affect the maximum electric field strength required for the initiation of upward leaders from wind turbine. A sample of a full-scale blade is shown in Figure 4. The design of the model used for analyzing full scale blade and a 3 meter blade tip section is shown below

Figure 4: V164-80m long wind turbine blade [16]

Figure 5 is a full-scale blade model design while figure 6 is the simulation.

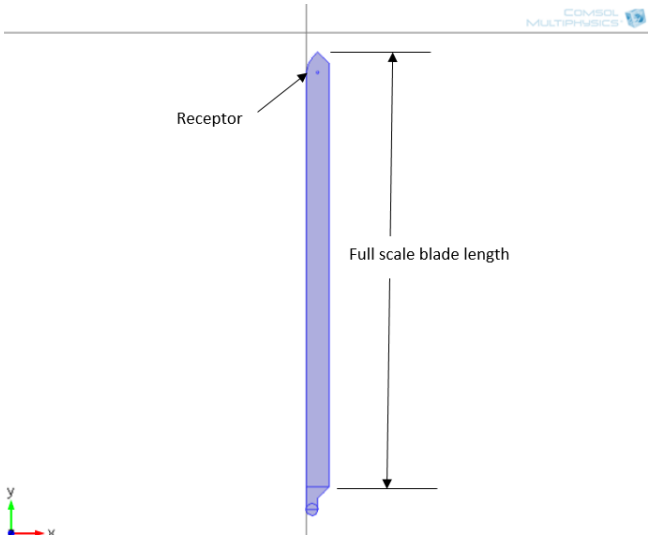

Figure 5: Full scale blade model

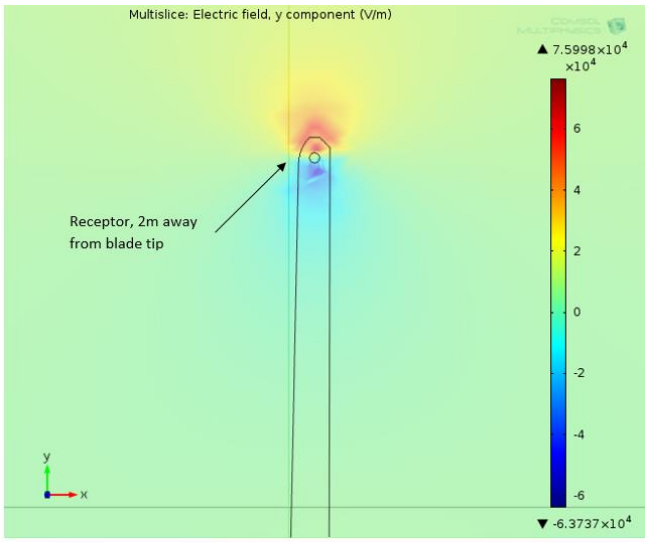

Figure 6: Full scale blade model simulation

a. 3 m blade tip section model

Figure 7 is a 3 m blade tip section model normally used for experimental analysis according to IEC 61400-24. Figure 8 is the simulation.

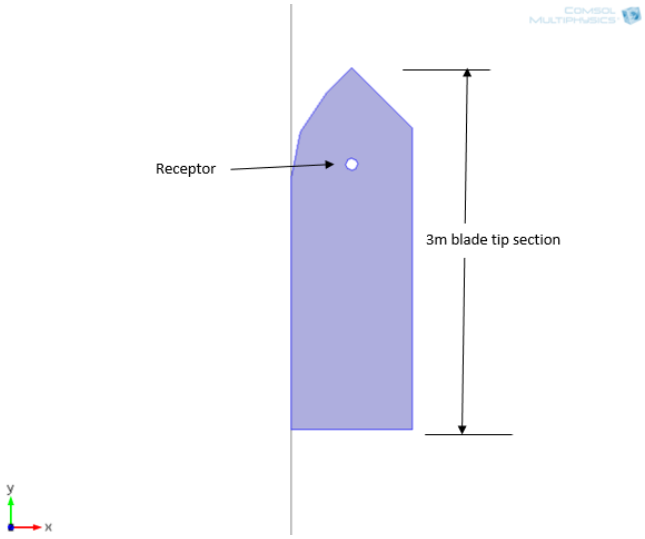

Figure 7: 3 m blade tip section model

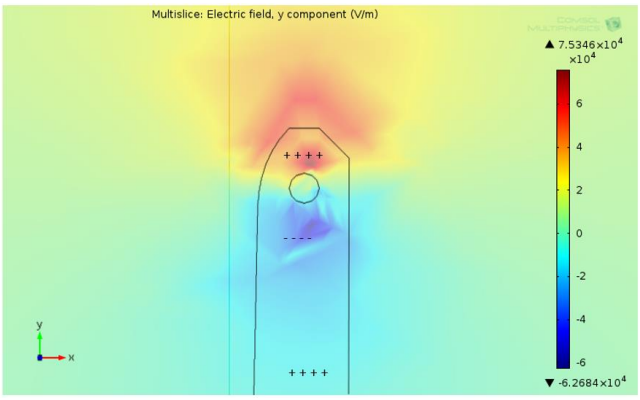

Figure 8: 3 m blade tip section model simulation

In the simulation, the wind turbine is protected by activating the receptor, field enhancement is observed at certain positions as shown. The level of electric field intensification is predominantly high around the lightning protection system of the wind turbine model and at the blade tip receptor. This intensification will allow the formation of upward streamers. From the figure, field enhancement is seen, it is apparent that upward leader will first incept from the blade in the vertical position. Lightning strike might initially attach to the lighting protection device depending on its ability to emit leader relative to the ability of the surrounding surface. Figure 9 shows the detailed activities around the receptor, these include; the upward positive polarity for streamer activities, the negative polarity going to ground through ground wire, positive polarity on the blade surface. Also shown is the produced corona charge (qc) which lowers the electric field on the tip inhibiting the occurrence of a streamer.

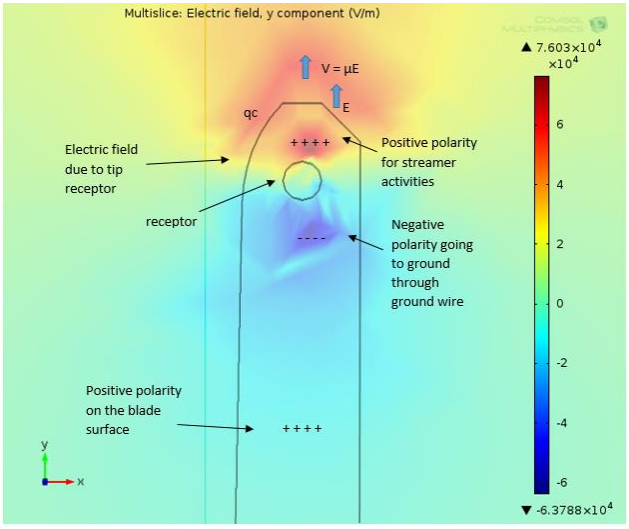

Figure 9: Activities around the receptor preceding leader initiation [12]

When lightning attaches to the receptor, it will be conducted to ground through ground wire without causing damage to the turbine. This is the intent of the lightning protection designer. If lightning is attached to the blade surface instead of the receptor, the blade and even the entire wind turbine can be destroyed. The focus is on evaluating the efficiency of the lightning protection systems by obtaining the maximum electric field strength required for the initiation of upward leader due to thunder cloud charge. The positions with higher electric field strength are considered to have higher possibility of inception of upward leader. The negative polarity going to ground through ground wire as shown in Figure 9 is usually confined to the ground wire and not on the surface of the blade, therefore, only the positive parts of the electric field strength are relevant. The most efficient situation in this analysis is the one with highest electric field on the receptor and minimum at the tip, leading edge, trailing edge and the entire blade surface, in this case, proficiency and failure of receptor is determined.

2.5. **Model for analyzing rotation**

The model used for rotation mode is shown in Figure 10. Blade A is moved counterclockwise for analyzing rotation. The evaluation is done as the blade is rotated through -60^0, -55^0, -50^0, -45^0, -40^0, -35^0, -30^0, -25^0, -20^0, -15^0, -10^0, -5^0, 0^0, 5^0, 10^0, 15^0, 20^0, 25^0, 30^0, 35^0, 40^0, 45^0, 50^0, 55^0 and 60^0 from the vertical position

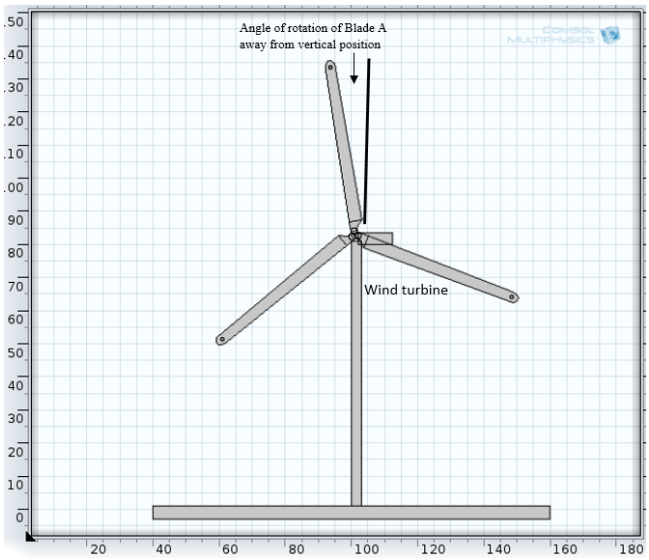

Figure 10: Rotation model

Figure 11 shows the simulation for the rotated blade. The maximum electric field strength required for the initiation of upward leader from the wind turbine is found to change as the blade is rotated.

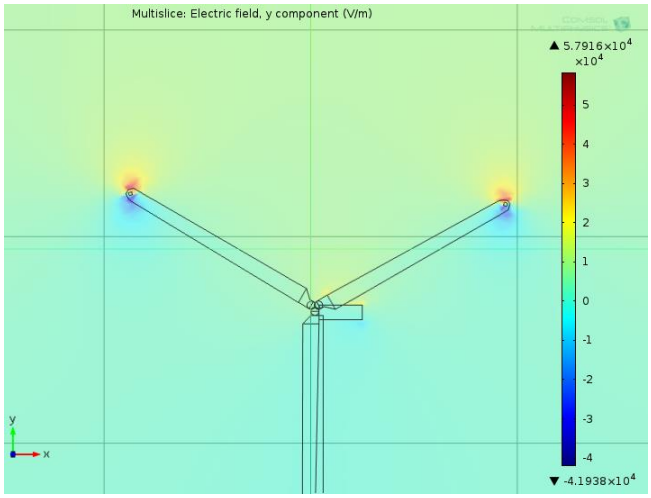

Figure 11: Rotated model simulation

Figure 12 shows the maximum electric field distribution as blade A is rotated from -60^0 to $+60^0$ from the vertical position: (a) 30^0; (b) vertical position; (c) -30^0; (d) 60^0; and (e) -60^0. It is generally observed that the electric field strength at the tip region appears to be higher than that at the inboard region. This is corroborative of laboratory experiments and field observations indicating that the tip is more exposed

than other part [17], and that upward leader is more likely to initiate from the tip receptor.

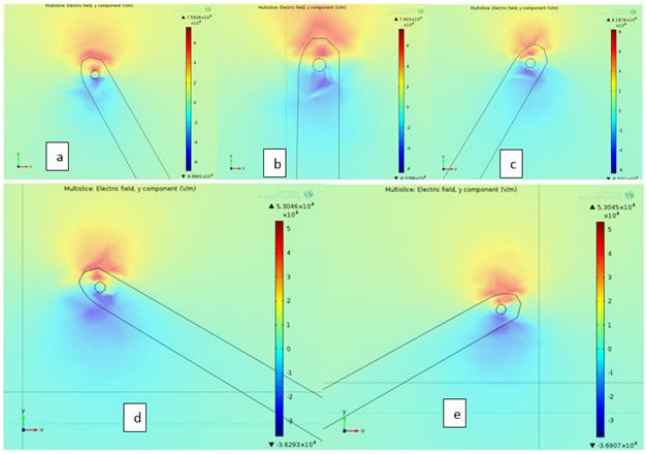

Figure 12: Maximum electric field distribution as blade A is rotated from -60 to +60 degrees from the vertical position: (a) 30; (b) vertical position; (c) -30; (d) 60; and (e) -60.

2.6. Model for analyzing receptor positions

The position of the receptor on the wind turbine or the blade greatly affects it performance. There are no standards as well as detailed experimental and numerical research covering receptor location. In this section, by comparing the electric field strength as the receptor position is changed and the blade is rotated, the receptor position can be evaluated and optimized. Figure 13 shows the discrete receptor position model. Four different configurations of receptor positions Figure 14 are applied on the wind turbine to investigate the effect of receptor position on initiation of upward leader. In the configurations, the receptor (10 mm in diameter) is fixed at discrete positions from the blade tip. These positions are 2 m, 1.5 m, 1 m and 0.6 m respectively. In each case, the evaluation is done as the blade is rotated through -60^0, -30^0, 0^0, 30^0 and 60^0 from the vertical position. Values are obtained from the blade tip, leading edge, trailing edge and the receptor tip.

The focus is on evaluating the efficiency of the receptor by obtaining the maximum electric field strength required for the initiation of upward leader due to thunder cloud charge.

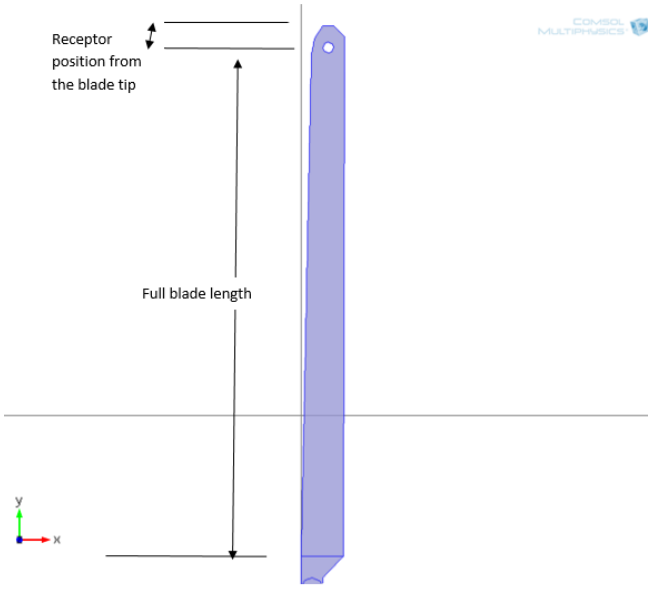

Figure 13: Discrete receptor position model

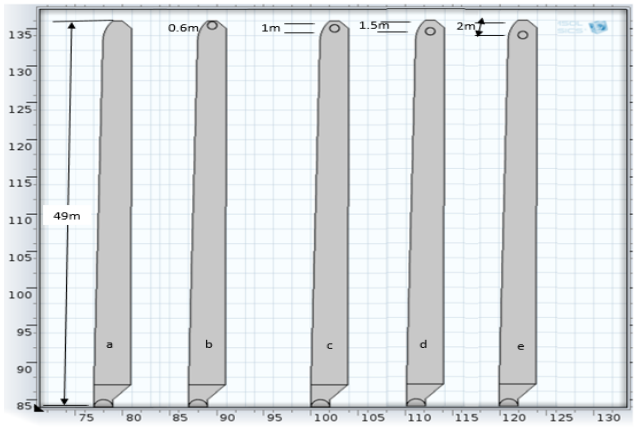

Figure 14: Different configurations of receptor positions from the blade tip used in the study: (a) No receptor; (b) 0.6 m; (c) 1 m; (d) 1.5 m; and (e) 2 m.

In order to investigate the effect of receptor position on the electric field strength, the simulation is first conducted on the wind turbine without the receptor and then the receptors are used on discrete positions as the blades are rotated. The simulation on the model for evaluating receptor position is shown below for the wind turbine and also for the blade in figure 15 and figure 16. The analysis is same for all models

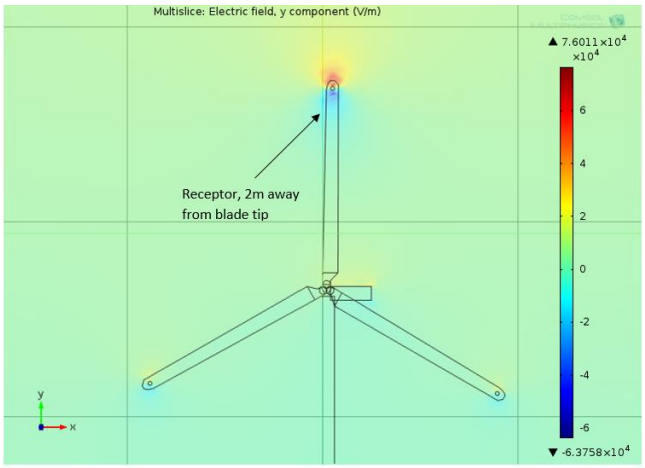

Figure 15: Wind Turbine simulation

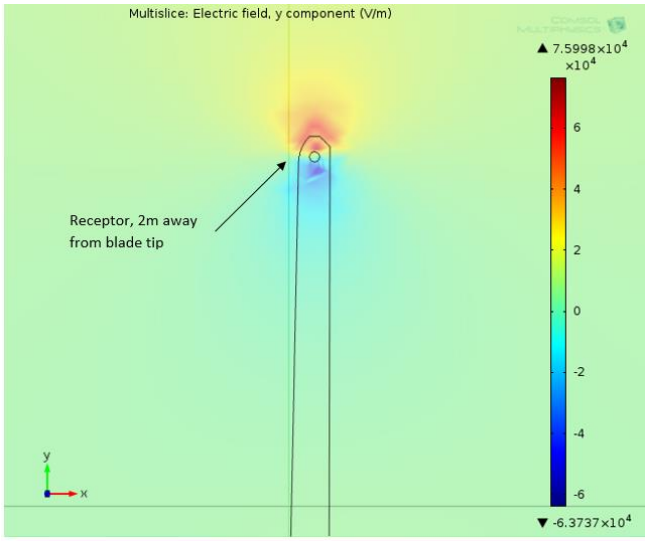

Figure 16: Blade simulation

2.7. Model for analyzing receptor sizes

The size of the receptor can influence the maximum electric field strength required for the initiation of upward leader from wind turbine. In this section, the model for analyzing receptor sizes is presented. Receptor sizes are investigated to know the best size. The receptor though effective [18], also failed in many instances [19, 20]. The efficiency of the receptor is dependent on its interception proficiency which is its ability to intercept a lightning stroke. This strongly dependents on the size of the receptors [21]. Since there are no standard governing receptor sizes, choices are made randomly by researchers. For instance; Abd-Elhady et al. [22], used 20 mm diameter, Wang et al. [23], used 0.2 m and 0.3 m radius, Naka et al. [24], used 25 mm diameter, in IEC61400-24, 15 mm diameter was applied, Peesapati and Cotton [15], used 10 mm diameter, Minowa et al. [25], used 20 mm diameter, Shindo et al. [18], used 35 mm in diameter, Yokoyama et al. [26], used 25 mm diameter and Danoon et al. [27], used 30 mm diameter. This non uniformity is not healthy for an efficient lightning protection because the results are affected as the size of the receptor has been found to significantly affect its efficiency. It is therefore necessary to harmonize on the most efficient receptor size for an efficient lightning protection of wind turbines. In this section, a model is presented for analyzing receptor size and their corresponding proficiencies. On this model, the receptor size can be evaluated and optimized by comparing the electric field strength as the receptor size is changed and the blade is rotated. Six receptor sizes (10 mm, 15 mm, 20 mm, 25 mm, 30 mm and 35 mm receptor diameters), encompassing adopted sizes in literature is applied here. The point of upward leader inception is predicted by the magnitude of the electric field strength. Figure 17 shows six receptor sizes applied on the wind turbine model to investigate the effect of receptor size on initiation of upward leader. In each case, the blade is rotated through -60^0, -30^0, 0^0, 30^0 and 60^0 from the vertical position. The rotation is useful in evaluating the influence of blade position on every part of the blade such as tip, leading edge, trailing edge and the entire blade surface. Also, rotation is responsible for dynamism and charge mobility. The receptor is placed 1.5 m from the blade tip as recommended [28]. The blade in the vertical position in Figure 10, is referred to as blade A. Values obtained from the blade tip, leading edge, trailing edge and the receptor tip for blade A only are considered and presented.

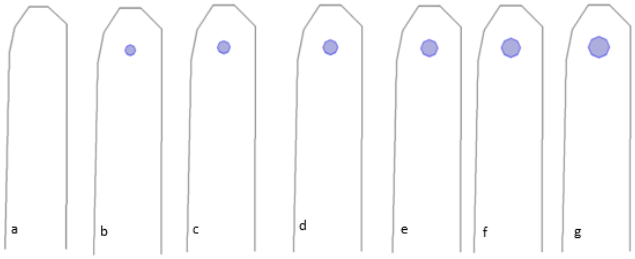

Figure 17. Different receptor sizes: (a) No receptor (b) 10 mm; (c) 15 mm; (d) 20 mm; (e) 25 mm; (f) 30 mm and (g) 35 mm diameters

Figure 18 shows the simulation for different receptor sizes used in the comparison of the maximum electric field strength distribution: (a) 10 mm; (b) 15 mm; (c) 20 mm; (d) 25 mm; (e) 30 mm and (f) 35 mm diameters respectively. The analysis is same as with other models above

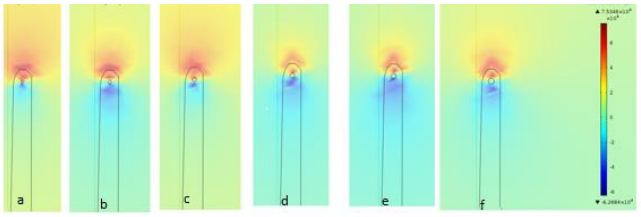

Figure 18. Receptor sizes and their various maximum electric field strength distribution: (a) 10mm; (b) 15 mm; (c) 20 mm; (d) 25 mm; (e) 30 mm and (f) 35 mm diameters respectively

2.8. Model for analyzing air termination systems

Here, the model for analyzing air termination systems is presented.

(1) Receptor: A disk type receptor made of copper (conductivity: 6.0×10^{-7}S/m), 10 mm in diameter, inserted at 1.5 m away from the blade tip [28], and connected to ground. This is shown in Figure 19.

(2) Metallic cap: In this system, 150 mm tip part of the blade is completely covered with copper foil and connected to ground, the metallic cap is shown in Figure 20.

(3) Performance enhancement method: In the performance enhancement method [29], the performance of the metallic cap was improved by adding a receptor at the middle of the blade. The model is shown in Figure 21.

Apart from the methods mentioned above, there are other methods such as metallic mesh, backside electrode, etc. these other methods can also be designed the same way.

The protection systems are connected to the down conductor inside the blade shell.

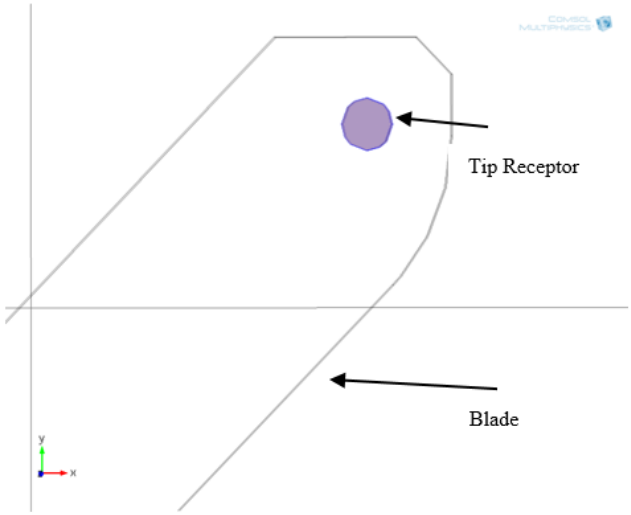

Figure 19. Tip receptor design

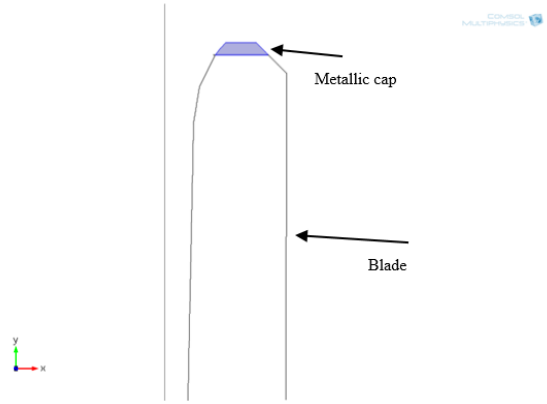

Figure 20. The metallic cap design

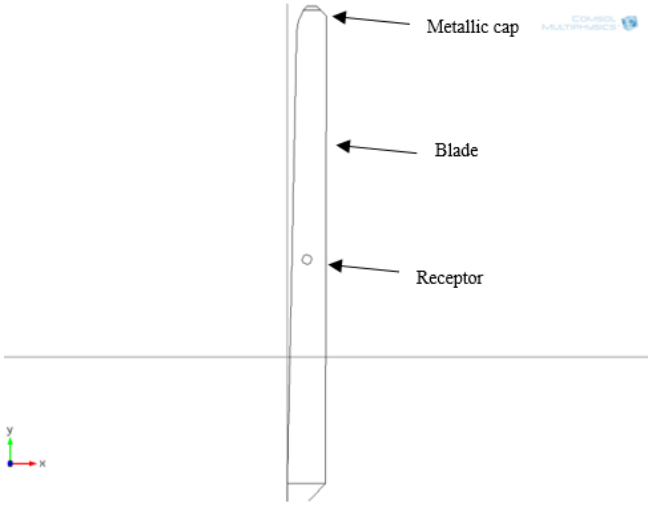

Figure 21. Enhanced method

The simulation for the receptor method, the metallic cap method and the enhanced method are shown below in Figure 22, 23 and 24. The enhanced method is shown in all the rotated position. The analysis is same as with other models above.

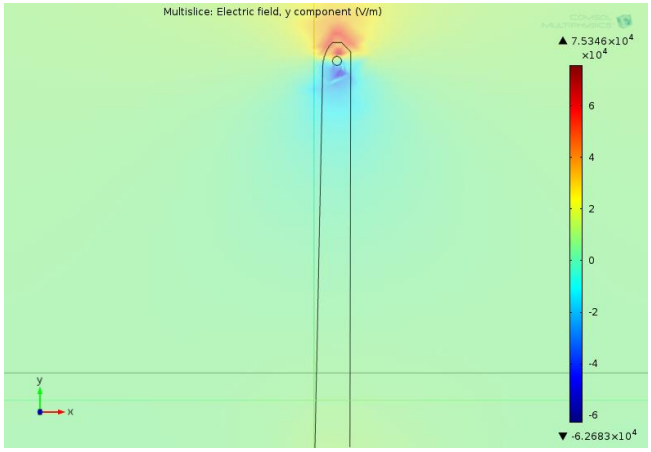

Figure 22. Receptor method simulation

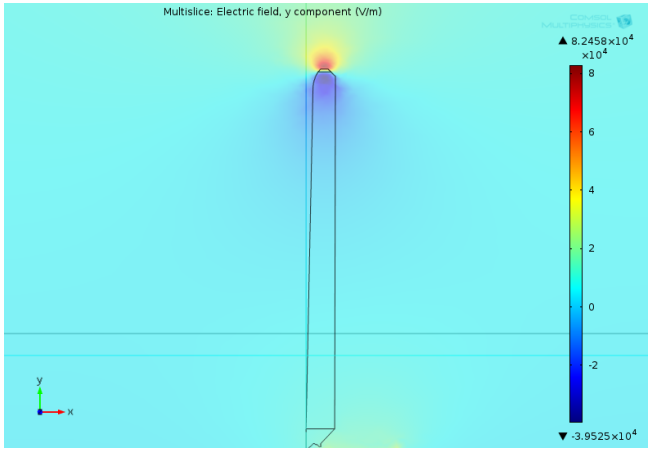

Figure 23. Metallic cap method simulation

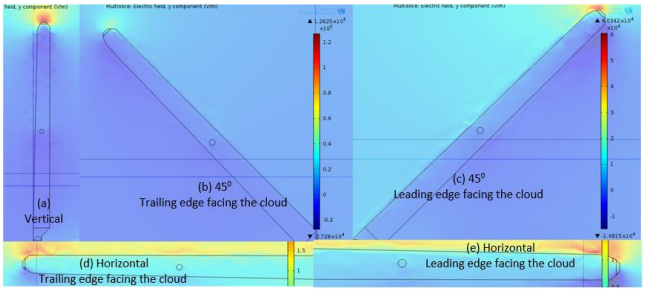

Figure 24: Enhanced method shown in all the rotated position

2.9. Model for analyzing polluted blade surface

Pollution of the blade can influence the maximum electric field strength required for the initiation of upward leader from wind turbine. Winds are stable and strong at the ocean owing to the absence of structures blocking the wind. When wind turbine is located offshore and in contact with salt water, it gets polluted with salt deposit which causes its insulation strength to decrease and raising the conductivity which could result in the blade going into competition with the receptors for lightning attachment. The problem with this is that Streamers can propagate from the surface of the blade instead of the receptors and as an unintended lightning part, the blade is severely damaged when hit by lightning and puncture of the blade can occur. This is a major problem for the wind industry. As compared to unpolluted blade surface, the conductivity as well as the relative permittivity are increased as observed from the distributed electric potential on the surrounding air and the blade surface. The simulation for polluted blades condition is done with values of the conductivity of the blades at 0.9 S/m and relative permittivity 80, this corresponds to the value of salt-water [24], the relative permittivity for normal water is higher than this value. The simulated polluted wind turbine model is shown in figure 24. The analysis with the polluted model is same as with other models above.

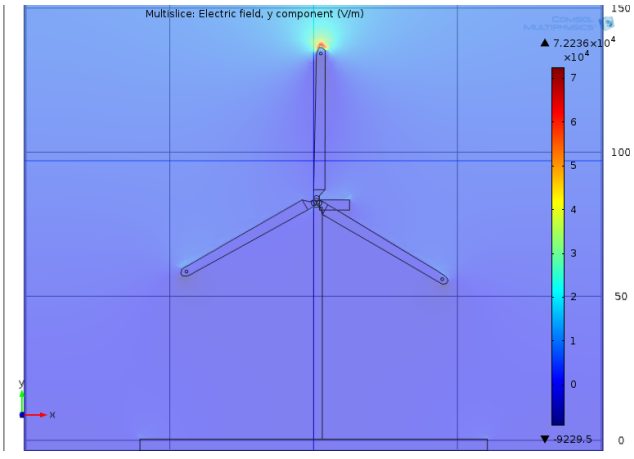

Figure 25. Polluted wind turbine

3. Conclusion

Multibody dynamic modelling of complex wind turbine blade lightning protection systems has been presented. Models are designed and analyzed and then proposed for complex multibodies of various blade conditions that can affect the inception of upward leader from wind turbines. Dynamically, the blades are rotated. The proposed models include; model for analyzing thunder cloud, model for analyzing wind turbine, model for analyzing full scale blade, model for analyzing full scale wind turbine, model for analyzing 3 m blade tip, model for analyzing receptor sizes, model for analyzing receptor position on the blade, model for analyzing various air terminal, model for analyzing rotation and model for analyzing polluted blade surfaces. The vertical tri-pole cloud charge distribution model is adopted using comsol multiphysics and then evaluated with high voltage strike attachment test. Results are accurate when validated experimentally and could be adopted for future and more complex shapes and structures. Further work shall include model for analyzing nacelle and other parts of the wind turbine.

References

1.Durstewitz, M., et al., *External conditions for wind turbine operation-results from the German'250 MW wind'programme*, in *European Union Wind Energy Conference*. 1996.

2.Zavareh, H.T., *Wind turbines protection against the lightning struck using a combined method*, in *Second Iranian Conference on Renewable Energy and Distributed Generation (ICREDG)*. 2012: Iran. p. 51-54.

3.Minowa, M., et al., *A study of lightning protection for wind turbine blade by using creeping discharge characteristics*, in *International Conference On Lightning Protection (ICLP)*. 2012. p. 1-4.

4.Ayub, A.S., W.H. Siew, and S.J. MacGregor, *Lightning protectionofwindturbineblades–Analternativeapproach*, in *7th Asia-Pacific International Conference*. 2011. p. 941-946.

5.Godson, I., et al., *Receptor Sizes and Its Effect on Lightning Protection of Modern Wind Turbines.* Journal of Green Engineering,, 2017. **Vol. 7 -3**: p. 401–420.

6.Staszewski, Ł., *Lightning Phenomenon–Introduction and Basic Information to Underst and the Power of Nature*, in *International Conference Environment and Electrical Engineering*. 2010: University of Technology, Wroclaw, Poland.

7.Wang, D., et al., *Observed characteristics of upward leaders that are initiated from a windmill and its lightning protection tower.* Geophysical Research Letters, 2008. **35**(2).

8.Rachidi, F., et al., *A review of current issues in lightning protection of new-generation wind-turbine*

blades. Industrial Electronics, IEEE Transactions on, 2008. **55**(6): p. 2489-2496.

9.Montanyà, J., O. Velde, and E.R. Williams, *Lightning discharges produced by wind turbines.* Journal of Geophysical Research: Atmospheres, 2014.

10.Zhou, H., et al., *Measured current and close electric field changes associated with the initiation of upward lightning from a tall tower.* Journal of Geophysical Research: Atmospheres, 2012. **117**(D8).

11.Godson, I., et al., *Optimum Receptor Location for Efficient Lightning Protection of Modern Wind*

Turbines International Journal of Simulatuion; Systems, Science and Technology ijssst, 2017.

12.Godson I. Ikhazuangbe, et al., *Upward Initiated Lightning Interactions with Wind Turbines using the Extended Vertical Tri-Pole Cloud Charge Distribution Model* European Journal of Science, Innovation and Technology EJSIT 2025. **5**(2): p. 279-302.

13.Rakov, V.A. and M.A. Uman, *Lightning: physics and effects*. 2003: Cambridge University Press.

14.Bazelyan, E.M. and Y.P. Raizer, *Lightning physics and lightning protection*. 2000: CRC Press.

15.Peesapati, V. and I. Cotton. *Lightning protection of wind turbines—A comparison of real lightning strike data and finite element lightning attachment analysis*. in *Sustainable Power Generation and Supply, 2009. SUPERGEN'09. International Conference on*. 2009. IEEE.

16.Vestas. Available from: http://www.windpoweroffshore.com/article/1211179/vestas-begins-testing-first-v164-80-metre-blade.

17.Peesapati, V., et al., *Lightning protection of wind turbines–a comparison of measured data with required protection levels.* IET renewable power generation, 2011. **5**(1): p. 48-57.

18.Shindo, T., A. Asakawa, and M. Miki, *Characteristics of lightning strikes on wind turbine blades. Experimental study of the effects of receptor configuration and other parameters.* Electrical Engineering in Japan, 2011. **176**(3): p. 8-18.

19.Yoh, Y. and Y. Shigeru. *Proposal of lightning damage classification to wind turbine blades*. in *Lightning (APL), 2011 7th Asia-Pacific International Conference on*. 2011. IEEE.

20.Yokoyama, S. *Lightning protection of wind turbine generation systems*. in *Lightning (APL), 2011 7th Asia-Pacific International Conference on*. 2011. IEEE.

21.61400-24, I., *Wind turbine - Part 24: Lightning protection*. 2010.

22.Abd-Elhady, A.M., N.A. Sabiha, and M.A. Izzularab, *Experimental evaluation of air-termination systems for wind turbine blades.* Electric Power Systems Research, 2014. **107**: p. 133-143.

23.Wang, Y. and W. Hu, *Investigation of the Effects of Receptors on the Lightning Strike Protection of Wind Turbine Blades.* IEEE Transactions on Electromagnetic Compatibility, 2017.

24.Naka, T., et al., *Experimental studies on lightning protection design for wind turbine blades.* Proceedings of Euro-pean Wind Energy Association (EWEC), Athen, Greece, 2006.

25.Minowa, M., et al. *A study of lightning protection for wind turbine blade by using creeping discharge characteristics*. in *Lightning Protection (ICLP), 2012 International Conference on*. 2012. IEEE.

26.Yokoyama, S., *Lightning protection of wind turbine blades.* Electric Power Systems Research, 2013. **94**: p. 3-9.

27.Danoon, L., A. El- Makadema, and A. Brown, *On the integration of lightning protection with stealth coated wind turbine blades.* Wind Energy, 2013.

28.Godson, I., et al., *Optimum receptor location for efficient lightning protection of modern wind turbines.* International Journal of Simulation Systems, Science & Technology, 2017. **18**.

29.Godson, I., et al., *Effect Of Pollution On Offshore Wind Turbine Blade Lightning Protection Systems.* Journal of Multidisciplinary Engineering Science and Technology (JMEST), 2019. **6**(4): p. 9858-9864.